Paper:
Malki, R., Masters, I., Williams, A. & Nick Croft, T. (2014). Planning tidal stream turbine array layouts using a coupled blade element momentum – computational fluid dynamics model. *Renewable Energy, 63*, 46-54.

http://dx.doi.org/10.1016/j.renene.2013.08.039

Elsevier Editorial System(tm) for Renewable Energy

Manuscript Draft

Manuscript Number:

Title: Planning Tidal Stream Turbine Array Layouts Using a Coupled Blade Element Momentum - Computational Fluid Dynamics Model

Article Type: Research Paper

Keywords: tidal stream; marine current; turbine array; CFD; blade element momentum theory

Corresponding Author: Dr. Rami Malki,

Corresponding Author's Institution:

First Author: Rami Malki

Order of Authors: Rami Malki; Ian Masters; Alison J Williams; T N Croft

Abstract: A coupled blade element momentum - computational fluid dynamics (BEM-CFD) model is used to conduct simulations of groups of tidal stream turbines. Simulations of single, double and triple turbine arrangements are conducted first to evaluate the effects of turbine spacing and arrangement on flow dynamics and rotor performance. Wake recovery to free-stream conditions was independent of flow velocity. Trends identified include significant improvement of performance for the downstream rotor where longitudinal spacing between a longitudinally aligned pair is maximised, whereas maintaining a lateral spacing between two devices of two diameters or greater increases the potential of benefitting from flow acceleration between them. This could significantly improve the performance of a downstream device, particularly where the longitudinal spacing between the two rows is two diameters or less. Due to the computational efficiency of this modelling approach, particularly when compared to transient computational fluid dynamics simulations of rotating blades, the BEM-CFD model can simulate larger numbers of devices. An example of how an understanding of the hydrodynamics around devices are affected by rotor spacing can be used to optimise the performance of a 14 turbine array is presented. Compared to a regular staggered configuration, the total power output of the array was increased by over 10%.

Highlights

- for a longitudinally spaced pair of turbines, the downstream device will have a lower performance even at 40 diameters' spacing because wake recovery is slow.
- for a low lateral spacing between a pair of turbines (3 diameters or less), flow recovery is slow between them because of wake expansion.
- flow acceleration between a pair of laterally spaced turbines can improve the performance of a third device positioned further downstream but laterally between them.
- the most benefit from such flow acceleration is gained by minimising the longitudinal spacing between the two rows of devices.
- for a small lateral spacing, performance of the downstream device is compromised.
- based on the patterns observed for two and three turbine arrangements, the overall performance of a 14 turbine staggered array was improved by over 10%.

Planning Tidal Stream Turbine Array Layouts Using a Coupled Blade Element Momentum - Computational Fluid Dynamics Model

[*]*Rami Malki, Ian Masters, Alison J. Williams and T. N. Croft*
Marine Energy Research Group, College of Engineering, Swansea University
Swansea, UK

[*]corresponding author: Rami Malki. tel: +44 (0) 1792 606 612. fax: +44 (0) 1792 295 676. e-mail: r.malki@swansea.ac.uk

word count: 5,807 plus references.

ABSTRACT

A coupled blade element momentum - computational fluid dynamics (BEM-CFD) model is used to conduct simulations of groups of tidal stream turbines. Simulations of single, double and triple turbine arrangements are conducted first to evaluate the effects of turbine spacing and arrangement on flow dynamics and rotor performance. Wake recovery to free-stream conditions was independent of flow velocity. Trends identified include significant improvement of performance for the downstream rotor where longitudinal spacing between a longitudinally aligned pair is maximised, whereas maintaining a lateral spacing between two devices of two diameters or greater increases the potential of benefitting from flow acceleration between them. This could significantly improve the performance of a downstream device, particularly where the longitudinal spacing between the two rows is two diameters or less. Due to the computational efficiency of this modelling approach, particularly when compared to transient computational fluid dynamics simulations of rotating blades, the BEM-CFD model can simulate larger numbers of devices. An example of how an understanding of the hydrodynamics around devices are affected by rotor spacing can be used to optimise the performance of a 14 turbine array is presented. Compared to a regular staggered configuration, the total power output of the array was increased by over 10%.

Keywords: tidal stream; marine current; turbine array; CFD; blade element momentum theory

INTRODUCTION

If the UK is to meet its Carbon reduction targets, for which a minimum reduction of 80 % by 2050 is required compared to 1990 levels as set out in the Climate Change Act 2008 [1], there needs to be a much more significant emphasis on reducing reliance on fossil fuels and placing a greater emphasis on renewable energy sources for power generation. There are numerous viable renewable energy sources that could be feasibly exploited to meet this goal [2], and considering the highly ambitious targets at hand, all such options will have to be considered. The focus of this work is on the tidal stream option, particularly beyond the initial prototyping and development stage which a number of developers are currently performing.

The UK is fortunate to have one of the best tidal resources in the world, capable of producing an estimated 16.3 TWh/year, which is equivalent to 4.2 % of the UK electricity production in 2008 [3]. However, to generate power at this scale, devices will have to be deployed in large numbers. Considering that the few trials on record to date have involved single or few devices, this raises many uncertainties regarding inter-device interaction within the context of a multiple turbine array. The lack of understanding of tidal stream devices and their performance in the natural environment has proven on numerous occasions to be costly, both in terms of time and resources as demonstrated by the

failures of the Atlantis device in Orkney, the Marine Current Technology device (SeaGen) in Strangford Lough and the OpenHydro device in the Bay of Fundy shortly after deployment, all of which involved blade failures. This lack of understanding is in part attributed to the complex and unfamiliar operating environment, but also to the novelty of the emerging technologies. This is where science and experience can be applied to inform the industry to minimise such risks in the future and support the marine energy industry.

Despite obstacles in developing the necessary technology and in gaining governmental consent for deployments, tidal stream power generation has emerged in recent years as a potentially reliable form of renewable energy due to the predictability of tide times and magnitudes as well as high concentration of the resource around the UK. Depending on the outcomes of trial deployments currently underway, it is likely that tidal stream deployments will occur at an accelerating rate over the coming decades. To date, a limited number of studies, both experimental and physical, have been performed to aid our understanding of how such deployments are likely to perform.

In terms of experimental studies, Myers and Bahaj [4,5] used porous disks to simulate tidal stream turbines in a practical study conducted in a laboratory flume. A range of lateral spacing between devices were assessed before a third disc was introduced further downstream effectively simulating a two-row turbine array. The hydrodynamics downstream of the discs were monitored. There are limitations to the use of porous disks to simulate rotating turbine blades, particular in the near region close to a turbine. However, the authors argue that the porous disks model provides a better representation of turbine wake hydrodynamics at small scales implemented in laboratory flumes where the rotor is less than 0.8 m in diameter due to problems with scaling. On the other hand, Mason-Jones et al. [6] show that non-dimensional rotor performance parameters (power, torque and thrust coefficients) for a tidal stream turbine are independent of scale and validate their model against a single 0.8 m diameter turbine. Nevertheless, the Myers and Bahaj [4,5] studies are some of the few with published data for simulations of multiple turbine arrays with downstream wake characteristics presented and are used to validate the model as presented in Masters et al. [7].

One of the simplest models used for evaluating turbine blade performance implements blade element momentum theory where tabulated hydrofoil data is used to determine lift and drag forces exerted by the blades onto the flow [8]. However, for evaluating multi-turbine arrays, any approach for rotor representation must be combined with a CFD solver to account for the influence of the turbines on the far-field flow structure as this will affect the performance of neighbouring turbines.

Numerical studies on turbine arrays have varied in complexity, ranging from the introduction of additional source terms to models based on solving the shallow-water equations and evaluating the large-scale effects of a turbine array on the environment, to more detailed CFD modelling of rotating turbine blades. For instance, Neill et al. [9] implements an additional bed friction term to a three-dimensional hydrodynamic model, POLCOMS, to simulate a 300 MW array positioned within the Alderney race. The influence of the array on morphodynamics is identified raising a need for careful planning to minimise environmental change. Similarly, Ahmadian et al. [10] modelled an array of turbines using a two-dimensional depth-integrated model whereby the turbines are represented through the addition of thrust and drag forces due to the turbine and supporting structure respectively. Effects of the array on water levels, tidal currents and water quality are predicted by the model. Ahmadian & Falconer [11] used the same model to evaluate the effects of array shapes concluding that denser arrays had more significant, but localised effects on water level and suspended sediment concentration. The significance of interaction between devices within an array setting was highlighted.

Turnock et al. [12] used a coupled model combining blade element momentum theory to represent blade forces on the flow and CFD to simulate flow through the domain to predict the hydrodynamics and performance of a single device. The authors recommend a 6×10^6 element mesh with 40 % of the

elements in the wake region for modelling a single rotor to achieve convergence. The requirement for minimising lateral spacing whilst maximising longitudinal spacing to achieve optimum power outputs by the array was identified. The authors predict power outputs of multiple turbine arrays by assuming that the power generated by consecutive rows reduces by a constant factor.

More detailed blade modelling was conducted by O'Doherty et al. [13], who simulated a five-turbine array using CFD modelling and identified fluid acceleration around devices which may be used to improve the performance of other turbines further downstream. The authors identified the usefulness of CFD models in improving the design. Also, Wang and Müller [14] conducted CFD simulations using FLUENT of ducted composite material marine current turbines. Each device consisted of a composite wheel, a nozzle and a diffuser. Groups of up to seven devices were considered arranged in three rows. The authors have identified the importance of careful selection of the array arrangement to optimise blockage of the flow and hence, maximise the power output of the array.

The studies published have either focused on over-simplified methods for rotor representation where the main purpose was to reproduce the general effect of the turbines on the flow, or very detailed three-dimensional models that are much more computationally expensive but are able to predict the performance of a small number of turbines. Studies published to date lack detailed modelling of larger turbine arrays that are typical of future deployments. This is addressed here by using the coupled BEM-CFD approach to physically simulate large multi-turbine arrangements. Firstly however, inter-device interactions are evaluated to serve as a guide for choosing suitable arrangements for optimising overall array performance.

MODEL DESCRIPTION

The BEM-CFD Model

Governing Equations

The steady-state CFD model solves the Navier-Stokes Equations, which consist of the equations for mass continuity (1) and the conservation of momentum (2) whereby the fluid is treated as incompressible and turbulent.

$$\nabla.(\rho \underline{u}) = 0 \tag{1}$$

$$\nabla.(\rho \underline{u} u_i) = -\partial p/\partial x_i + \nabla.(\mu_{lam} + \mu_t)\nabla \rho u_i + S_i \tag{2}$$

In these equations, ρ is the fluid density, u_i is the i'th component of the velocity vector, p is the pressure, μ_{lam} and μ_t are the dynamic laminar and turbulent viscosities respectively and S_i represents additional source terms into the momentum equations. Turbulence in the flow is resolved using the k-ε model [15] in which (3) and (4) are solved:

$$\nabla.(\rho \underline{u} k) = \nabla.(\mu_{lam} + \mu_t/\sigma_k)\nabla k + \mu_t G - \rho\varepsilon \tag{3}$$

$$\nabla.(\rho \underline{u} \varepsilon) = \nabla.(\mu_{lam} + \mu_t/\sigma_\varepsilon)\nabla\varepsilon + \mu_t G - \rho\varepsilon + \varepsilon/k(C_{1\varepsilon}\mu_t G - C_{2\varepsilon}\rho\varepsilon) \tag{4}$$

(3) is the conservation equation for turbulent kinetic energy, k, and (4) is the conservation equation for the turbulent dissipation rate, ε. The turbulent viscosity, μ_t, is calculated using (3) and (4) as follows:

$$\mu_t = \rho C_\mu k^2/\varepsilon \quad (5)$$

In (3), (4) and (5), σ_k, σ_ε, $C_{1\varepsilon}$, $C_{2\varepsilon}$ and C_μ are constants for which standard values are used, and G is the turbulent generation rate.

Rotor Representation

For large time scales, the time-averaged influence of turbine blades on the flow is considered to act over all parts of a circular area with a diameter equal to that of the blade. Forces acting on the flow due to the blade are assumed to be equal across the circular area for equal radial distances from the centre. This time-averaged approach allows sources that represent the force on the fluid due to the blades of the turbines to be applied to each of the momentum equations. The advantage of this approach is that the physical characteristics of the blade are built into the source rather than the mesh consequently allowing the use of better quality meshes. The disadvantage is that because of the time average principle of the approach it fails to resolve any transient flow features due to blade position.
To define the characteristics of the rotor according to axial and radial position the blade element momentum (BEM) method is employed [8]. Fig. 1a shows diagrammatically how a three bladed rotor is discretised using the BEM approach. The blade properties for a blade element at a certain radius, r, are determined and are then averaged throughout the whole of the shaded region. This is performed for each blade element throughout the radius of the rotor, R.

Each blade element has a chord length, c, and radial width, δr. Each element experiences forces acting on it due to the fluid. These are shown in Fig. 1c. dT and dF_A represent the torque and axial forces respectively. The lift, dL, and drag, dD, are dependent on the angle of attack, α, between the blade element and the resultant velocity, v_R. Ω is the angular velocity of the turbine and U is the upstream longitudinal flow velocity. The angle of attack and flow inclination angle are denoted by α and ϕ respectively.

Following the approach described by Masters et al. [8], an axial force on a blade element is defined by:

$$F_A = F_L\sin\phi + F_D\cos\phi \quad (6)$$

and the tangential force on a blade element, which is equal to the torque/radius, i.e. dT/r, is defined by:

$$F_T = F_L\cos\phi - F_D\sin\phi \quad (7)$$

The flow inclination angle, ϕ, is defined by:

$$\phi = \tan^{-1}((\Omega r - u_\Theta)/u_z) \quad (8)$$

where u_Θ, u_z are the local fluid tangential and axial velocities respectively, and Ω is the angular velocity of the blades in rad/s. The lift force, dL, and drag force, dD, are given by:

$$dF_L = \rho|v_R|^2 C_L c dr/2 \quad (9)$$

$$dF_D = \rho|v_R|^2 C_D c dr/2 \quad (10)$$

Here, C_L and C_D are the lift and drag coefficients respectively, and:

$$|v_R|^2 = u_z^2 + (\Omega r - u_\Theta)^2 \quad (11)$$

Substituting (9) and (10) into (6) and (7) gives the following equations:

$$S_z = dF_A = \rho|v_R|^2 c dr(C_L \sin\phi + C_D \cos\phi)/2 \quad (12)$$

$$S_\Theta = dF_T = \rho|v_R|^2 c dr(C_L \cos\phi - C_D \sin\phi)/2 \quad (13)$$

which, when resolved into Cartesian components and converted into force per volume, are substituted into the momentum equations (2) through S_i.

A more detailed description of the model is presented in [16], including an assessment of the significance of mesh resolution within the blade-box region on the performance coefficients predicted by the model. The blade-box is defined as an allocated region of the model domain large enough to accommodate the turbine rotor and where the blade source terms are introduced and is characterised by a structured mesh even if the mesh throughout the rest of the domain is unstructured as this improves blade force representation.

In this study, simulations are conducted for a 10 metre diameter rotor, which is a reasonable representation of the scale of turbines likely to be deployed in offshore environments. The chord length and chord twist angle characteristics of the blade are presented in Fig. 2. These profiles are used to determine the occupation of the blades over the blade-box region to determine the exact location of the blade forces.

The model is capable of predicting the performance of turbine rotors as demonstrated in [16] where model results were compared against measured tow-tank data collected by [17]. Discrepancies in the model predictions of power coefficients compared to the experiment following blockage corrections were between -1.07 % and 7.95 % for tip speed ratios between 4.0 and 8.0. In [8], it was also shown that the model is capable of predicting velocity structures in the wake regions downstream of turbine rotors. Beyond two diameters downstream of rotors within arrangements of two and three devices, the maximum error observed along the mid-wake of any of the rotors was 11.38 %, but was often much lower.

In this study, a consistent TSR of 3.0 based on the local velocity at the rotor is implemented for all simulations conducted, and the associated errors will therefore be consistent.

Mesh dependency of the simulations within the blade-box and wake regions was assessed in [16] and [8] respectively. An 11.2 m × 11.2 m × 1.0 m blade-box was designated to contain the rotor source terms. Based on the recommendations in these previous studies, a structured mesh is employed in the blade box region with a resolution of 64 × 64 × 10 elements with cell sizes of 0.2 m × 0.2 m × 0.1 m. An unstructured mesh is implemented in the upstream regions with maximum element sizes of 1.0 m between -55 (55 m upstream of the turbine) m and 60 m (60 m downstream of the turbine), except the rotor vicinity of -5 m and 10 m where a maximum element size of 0.5 m was implemented. Beyond 60 m downstream of the rotor, a maximum element size of 2.0 m was implemented, and 4.0 m along the outer boundaries of the model domain.

CFD Solver Details

The computational fluid dynamics solver used in this work employs an unstructured mesh-finite volume discretisation procedure [18]. All variables are located at the centres of the mesh elements. This choice requires the use of non-linear interpolation to prevent spurious pressure oscillation in the

solution. In this context, the Rhie-Chow interpolation method [19] is used to calculate convective fluxes. The pressure-momentum coupling is effected through a variant of the SIMPLEC procedure. A bounded central differencing scheme [20] is used to evaluated the combined advection-diffusion contributions.

TURBINE ARRANGEMENTS

Using the BEM-CFD model outlined above, a number of tidal stream turbine arrangements are considered. First, a single 10 m diameter device in a rectangular channel is simulated with the aim of evaluating the wake structure developing downstream of a turbine rotor. The channel implemented in the model is 200 m wide (20 diameters) and 700 m long with upstream and downstream reaches of 300 m and 400 m respectively (see Fig. 3-a). A constant 30 m flow depth is maintained throughout the model domain with the rotor centred vertically within the water column and laterally across the domain. The width of the channel was chosen so as to increase the cross-sectional area of the domain and hence, reduce blockage effects that will arise as a result of the rigid lid nature of the model. Large stretches of channel were implemented both upstream and downstream of the rotor to improve flow structure development between the upstream boundary and the rotor, and to allow for an adequate distance between the rotor and the downstream boundary to assess wake development. Simulations were conducted for inlet velocities between 0.5 m s^{-1} and 3.0 m s^{-1}, which fall within the range of values observed in typical offshore environments where tidal stream turbines are likely to be deployed.

For the next part of this study, pairs of rotors are considered which were implemented in the same rectangular domain geometry described above. For pairs of rotors, the effects of longitudinal (Fig. 3-b) and lateral (Fig. 3-c) spacing on turbine performance are evaluated. Longitudinal spacing considered ranged between 5 and 30 diameter lengths whereas lateral spacing considered ranged between 1.5 and 5.0 diameters. Three-turbine arrays were then considered (Fig. 3-d) to evaluate the performance of the rotors in the context of turbine arrays.

SINGLE TURBINE

Average wake velocities were evaluated by calculating the area-mean velocity through a 10 m diameter circular region lateral to the flow direction, equivalent to the rotor area, and this was normalised by the inlet velocity value. A circular grid consisting of points separated by 10 degrees in the tangential direction and 1.0 m in the radial direction was created across each 10 m diameter circular region. The circular grid was replicated every 5.0 m in the longitudinal direction downstream of the rotor. Root mean square (RMS) velocities were interpolated onto the grid points and an area-mean was calculated for each circular grid. The resolution of the solution grid is variable with distance from the rotor and this was described earlier.

The resulting profiles are presented in Fig. 4. There was strong similarity between the profile shapes regardless of the magnitude of the inlet velocity. This differs from our findings regarding the dimensions of the wake edge [21] which is modified by the flow velocity. Following a significant decrease in normalised velocity immediately downstream of the rotor, a minimum velocity of between 37.8 % and 39.3 % of the inlet velocity is achieved 2.0 diameters downstream of the rotors. This is followed by a rapid velocity recovery up to 10 diameters downstream beyond which there is a gradual decrease in the rate of recovery. By 40 diameters downstream, the velocity recovered to around 92 % of the inlet velocity magnitude. This is in part a property of the smooth rectangular channel which may lead to lower levels of wake and turbulence dissipation than may be observed in more realistic environments with complex bottom bathymetries. However, these finding indicate that the influence

of a rotor on the flow along its wake can be observed at considerable distances downstream of the rotor. Although downstream velocity measurements were only recorded for distances of up to 25 diameters downstream of the porous disks used to simulate turbine rotors, even at this distance, influence of the disks on the flow can be detected. This should be accounted for when choosing locations for the deployment of further devices.

TWO TURBINES

For pairs of turbines aligned in the flow direction with longitudinal spacing up to 40 diameters between the upstream and downstream rotors, there was little difference in the velocity profile shapes downstream of the second rotor (Fig. 6). The minimum velocity occurred 0.5 diameters from the downstream rotor and ranged between 37.6 % for a spacing of 10 diameters and 46.7 % for 40 diameters. Recovery beyond this point resulted in very similar profiles.

Velocity profiles across and downstream of the upstream turbines were identical regardless of the longitudinal spacing between the pair of rotors. The velocity through the upstream rotor was 67 % of the freestream velocity, and a minima equal to 40 % of the free stream velocity was achieved 2.5 diameters downstream of the rotor. Flow through the downstream rotor was influenced significantly by the longitudinal spacing **(**Fig. 5**)** as this determined the extent of flow recovery before reaching the downstream rotor.

The velocity through the upstream rotor, and hence, its power output, was not affected significantly by the positioning of the downstream rotor (see Fig. 6). Performance of the downstream rotor improved significantly with increasing the longitudinal distance between the rotors, even when the spacing was 40 diameters. For a longitudinal spacing of 10 diameters, the predicted power output of the downstream rotor was 29.3 % of that of the upstream rotor compared to 82.8 % for a spacing of 40 diameters.

Turnock et al. [22] suggest that the power output of a rotor in any given row of a multiple row array will have a power output less than that of the rotor immediately upstream by factor specific to the entire array. Although this conclusion is very useful in terms of array planning, it is worthy of further investigation using a more direct modelling approach. The authors' conclusion was made based on the simulation of a single rotor, and there are many uncertainties as to what extent this relationship holds in the context of arrays that vary in numbers of rotors along their width, the longitudinal spacing of the devices within the array and the freestream velocity. The velocity profiles presented in Fig. 5 indicate that the velocity at a third device placed further downstream would not be affected by the longitudinal spacing between the first two devices, but would be affected by how far downstream the third rotor is placed.

Lateral spacing between rotors can affect the speed of flow recovery along the centreline between them in the downstream direction (see Fig. 7), which in turn can have implications on the performance on turbines further downstream within the context of a multiple row array. If the rotors are too close laterally in proximity (2.0 diameters or less), the cumulative obstruction of the two rotors to the flow becomes significant and can hinder velocities between them. For such lower velocities, flow recovery was slower, and at 40 diameters downstream, the flow velocity was predicted as 91 % of the freestream velocity for a lateral spacing of 2.0 diameters, and 86 % for 1.5 diameters. Increasing the lateral spacing between the rotors results in acceleration of the flow within the central region, and this results in velocities that are even higher than the freestream in the far downstream. This can be seen most clearly for lateral spacing of 4.0 diameters or greater where 40 diameters downstream, the flow velocity was around 4.0 % higher than the freestream velocity.

THREE TURBINES

The longitudinal and lateral spacing between rotors within an array can have a significant effect on the velocity and turbulence structures as shown in Fig. 8a and b respectively, which in turn can affect the performance of the rotors within the array. Turbulence intensity is estimated from the predicted velocity, U, and turbulent kinetic energy, k, as follows:

$$T_i = (2k/3)^{0.5}/U \quad (14)$$

The lateral and longitudinal spacing, in diameters, for plots i, ii, iii and iv are (1.5,1.0), (3.0,1.0), (1.5,10.0) and (3.0,10.0) respectively. Whereas a lateral spacing of 1.5 diameters between the upstream rotors results in the downstream rotor falling within their wakes and experiencing lower velocities, increasing the lateral spacing to 3.0 diameters results in the opposite effect and the downstream turbine falls within a higher velocity region resulting from flow acceleration occurring between the upstream rotors.

Smaller lateral spacing also results in the downstream turbine experiencing a more turbulent flow as indicated by the turbulence intensity contours. The turbulence intensity was greatest where the lateral spacing was small but the longitudinal spacing large. This can have further implications, not only on rotor performance, but also on the durability of its blades, however to evaluate this problem, more sophisticated modelling approaches are necessary involving fluid-structure interaction (FSI) analyses [23].

For a narrow spacing of 1.5 diameters between the upstream rotors, there is a clear reduction in centreline velocities whereby values between the two rows of turbines are below the freestream velocity (Fig. 9a) as was seen previously for the pair of laterally spaced rotors (Fig. 7). For the three-turbine array, this results in lower velocities approaching the downstream rotor which in turn will reduce the extractable power. For larger rotor separations, for instance 2.5 diameters as shown in Fig. 9b, there is an acceleration of the flow between the two rotors which leads to an increase in velocity magnitudes between the two rows, and the velocity upstream of the rear rotor is even higher than the freestream velocity which can improve its performance.

The influence of the arrangement of the three rotors had a less significant effect on the flow recovery beyond the downstream rotor (see Fig. 10). For larger lateral spacing between the upstream pair, the downstream velocity profiles were virtually identical regardless of longitudinal spacing. For a smaller lateral spacing of 1.5 diameters, flow recovery was slower for a smaller longitudinal spacing within the array. This will have further implications in the context of larger arrays whereby increasing the lateral spacing between turbines can have less of a compromise on the performance of devices arranged in rows further downstream.

Power output predictions for the downstream rotor within a three-rotor array are presented in Fig. 11. Variation in the predicted power output can be seen clearly with lateral and longitudinal spacing, particularly for lateral spacing below 3.0 diameters as the flow structure between the devices can be affected significantly by turbine spacing.

Regardless of the longitudinal spacing between the upstream and downstream rotors, performance of the downstream rotor was significantly compromised where the lateral spacing between the upstream rotors was 1.5 diameters. Having the devices in such close proximity of each other clearly resulted in a cumulative obstructive effect along the centreline between them, and this had a significant effect by reducing flow velocities in the far-downstream.

Increasing the lateral spacing between the upstream pair of rotors had a varied influence on the downstream rotor depending on longitudinal spacing. For lateral spacing of 3.0 diameters or greater, there was little variation in the power output of the downstream rotor with variations in longitudinal spacing, although reducing the longitudinal spacing resulted in benefiting from flow acceleration

between the two upstream devices and hence, slightly improving performance of the downstream rotor. However, for lateral spacing less than 3.0 diameters, there was a drop in performance of the downstream rotor with increasing longitudinal spacing and this may be attributed to wake expansion which affects velocities along the centreline of the array to a greater extent with increasing distance from the upstream pair of rotors, particularly when they are so closely spaced.

FOURTEEN TURBINES

Based on the findings of the work presented above on two and three turbine arrangements, an example is presented here demonstrating how such knowledge of interaction between devices can be utilised in designing array layouts to optimise performance. In Fig. 12a, a 14 turbine array arranged in 4 rows is simulated whereby the lateral and longitudinal spacing are 3.0 diameters and 10.0 diameters respectively. These arbitrary values have been chosen to reproduce reasonable turbine spacing that may be implemented in a real situation. Fig. 13c reports the power output of this configuration.

Turnock et al. [22] suggest that for a turbine array, the power output of consecutive rows can be predicted by applying a constant factor to the power output of the previous row upstream, although it is also suggested that this hypothesis is more applicable to turbines arranged in a regular square pattern. However, turbines are more likely to be deployed in staggered arrangements to maximise the performance of downstream devices, and the model results presented here indicate that the relationships between consecutive rows may be more complex and would require further investigation to prove such hypothesis. For instance, if one of the middle rotors from each of the first and third rows (rotors 2 and 9), and the middle rotors from the second and fourth rows (rotors 6 and 13) are considered, it is not possible to apply a constant factor for the prediction of downstream devices. Considering the rotors in ascending order (2, 6, 9 and 13), the multiplication factors required to predict the power outputs of rotors 6, 9 and 13 from the power output of the upstream rotor in each case would be 1.098, 0.658 and 0.967 respectively. Alternatively, predicting the power outputs of rotors 9 and 13 based on the next linearly upstream rotor (2 and 6) would require factors of 0.722 and 0.636. This indicates that in a large array layout, influence on the flow around a downstream device is likely to be much more complex and will be difficult to characterise using a simple empirical relationship, however, this would require further investigation. Other factors that will affect device performance in natural environments will include bathymetric effects, bottom roughness and variation in flow cross-sections which will make it even more difficult to propose such a standardised method for performance prediction.

The second simulation presented in Fig. 12b shows a different arrangement in which the lateral spacing between devices is increased to 4.0 diameters to maximise the flow acceleration between them. The second and third rows were moved so that they are one diameter away from the first and fourth rows such that the distance between the second and third rows is 38.0 diameters. This serves two purposes; firstly, the second and fourth rows will benefit from the flow acceleration between upstream rotors to a greater extent, and secondly, this facilitates a greater level of flow recovery before the flow interacts with the third and fourth rows.

For the original array layout, the predicted total power output was 7.7 MW, whereas for the modified arrangement, 8.5 MW were predicted corresponding to a 10.7 % increase in performance (Fig. 12c). Based on the lateral profiles of velocity downstream of three-rotor arrays presented above, the overall performance of the array may be improved further by offsetting the third and fourth rows so that rotors do not fall directly along the wakes of rotors within the first and second rows.

CONCLUSIONS

The BEM-CFD model implemented in this study is a computationally efficient method for simulating tidal stream rotors and capturing their influence on the far-field flow structure. Such efficiency, particularly when compared to the classical CFD modelling of flow around rotating turbine blades, makes the coupled BEM-CFD model a suitable method for modelling turbine arrays consisting of a relatively large number of rotors. Since the modelling approach accounts for the influence of rotors on their surrounding flow, it is capable of accounting for the interaction between devices and predicting the performances of individual devices within different array layouts.

Following a brief study of the hydrodynamics downstream of a single device, this paper progresses to consider the influence of numerous devices on each other and hence, the overall performance of a turbine array. A turbine array layout can most simply be characterised by two factors: firstly, whether the turbines are arranged in a regular or staggered arrangement, and secondly, the spacing between the devices, and this in turn can be considered in terms of lateral spacing between devices within the same row, or the longitudinal spacing between devices in consecutive rows. Both types of spacing were considered.

Longitudinal spacing up to 40 diameters between two rotors were considered, and even at largest spacing, the power output of the downstream device was 82.8 % of the upstream device, although performance of the downstream device improved dramatically with increasing longitudinal spacing. Flow recovery downstream of a rotor is likely to be affected slightly depending on the choice of turbulence model, and this was shown in a comparison between the most widely used two-equation models, namely the k-ε, k-ε RNG and the k-ω models [24]. More complex turbulence models should also be considered.

The lateral spacing between a pair of devices affected the rate of flow recovery downstream. It was shown that for a lateral spacing of 3.0 diameters or greater, there was little difference in downstream recovery, however, for smaller spacing, recovery was much slower. This will be of most relevance in the context of larger arrays where further devices may be placed downstream.

Large arrays are likely to be designed in staggered arrangements as this reduces wake interference between consecutive rows and increases the distance of flow recovery between every other row, or between longitudinally aligned devices. To evaluate the effects of rotor layouts on hydrodynamics within a staggered arrangement, a three-turbine array was modelled with various lateral spacing between an upstream pair of rotors and longitudinal spacing between them and a third rotor positioned downstream and centred between them. Performance of the downstream device was affected by both lateral and longitudinal spacing. For lateral spacing of 2.0 diameters or greater, flow acceleration occurred between the upstream rotors and the performance of the downstream rotor was maximised by reducing the longitudinal spacing to benefit from such flow acceleration. At 2.0 diameters however, downstream rotor performance was significantly compromised for longitudinal spacing greater than 2.0 diameters, and this can be attributed to expansion of the upstream wakes which at such small lateral spacing affects the location of the downstream rotor between them. For lateral spacing below 2.0 diameters, downstream flow recovery was extremely slow due to the magnitude of the combined obstruction to the flow created by the two rotors.

Finally, the BEM-CFD model was used to simulate a 14-turbine array and predict both the performance of individual devices within the array and the hydrodynamic flow structure between the rotors to demonstrate how this tool can be useful to developers in real projects. First, a standard hypothetical staggered arrangement of four rows with constant lateral and longitudinal spacing of 3.0 and 10.0 diameters respectively was modelled. Then the array layout was altered based on the observations from the evaluation of the influence of spacing between devices on performance. As a result, the overall array power output was increased by over 10 % which is a significant improvement that would improve the return on the investment.

REFERENCES

1. The Department of Energy and Climate Change. *Climate Change Act 2008*. The Stationary Office Limited 2008.
2. The Department of Energy and Climate Change. *UK Renewable Energy Roadmap*. The Stationary Office Limited 2011.
3. AEA. *Analysis of Renewables Growth to 2020*. 2010.
4. Myers L.E., Bahaj A.S. Simulated electrical power potential harnessed by marine current turbine arrays in Alderney Race. *Renewable Energy* 2005; **30** : 1713-1731.
5. Myers L.E., Bahaj A.S., *An experimental investigation simulating flow effects in first generation marine current energy converter arrays*. Renewable Energy 2012; **37** : 28-36.
6. Mason-Jones A., O'Doherty D.M., Morris C.E., O'Doherty T.O., Byrne C.B., Prickett P.W., Grosvenor R.I., Owen I., Tedds S., Poole R.J. *Non-dimensional scaling of tidal stream turbines*. *Energy* 2012; **44** : 820-829.
7. Masters I., Malki R., Williams A.J., Croft N. *The influence of flow acceleration on tidal stream turbine wake dynamics: a numerical study using coupled BEM-CFD model*. Computer Methods in Applied Mechanics and Engineering. (in press).
8. Masters I., Chapman J.C., Orme J.A.C., Willis M.R. *A robust blade element momentum theory model for tidal stream turbines including tip and hub loss corrections*. Journal of Marine Engineering and Technology 2011; **10**(1) : 25-35.
9. Neill S.P., Jordan J.R., Couch S.J. *Impact of tidal energy converter (TEC) arrays on the dynamics of headland sand banks*. Renewable Energy 2012; **37** : 387-397.
10. Ahmadian R., Falconer R., Bockelmann-Evans B. *Far-field modelling of the hydro-environmental impact of tidal stream turbines*. Renewable Energy 2012; **38** : 107-116.
11. Ahmadian R., Falconer R.A. *Assessment of array shape of tidal stream turbines on hydro-environmental impacts and power output*. Renewable Energy 2012; **44** : 318-327.
12. Turnock S.R., Phillips A.B., Banks J., Nicholls-Lee R. *Modelling tidal current turbine wakes using a coupled RANS-BEMT approach as a tool for analysing power capture of arrays of turbines*. Ocean Engineering 2011; **38** : 1300-1307.
13. O'Doherty T., Egarr D.A., Mason-Jones A., O'Doherty D.M. *An assessment of axial loading on a five-turbine array*. Proceedings of the Institution of Civil Engineers - Energy 2009; **162**(EN2) : 57-65.
14. Wang J., Müller N. *Performance prediction of array arrangement on ducted Composite Material Marine Current Turbines (CMMCTs)*. Ocean Engineering 2012; **41** : 21-26.
15. Launder B.E., Spalding D.B. *Mathematical models of turbulence*. Academic Press, London. 1972.
16. Malki R., Williams A.J., Croft T.N., Togneri M., Masters I. A Coupled Blade Element Momentum - Computational Fluid Dynamics for Evaluating Tidal Stream Turbine Performance. Applied Mathematical Modelling (in press).
17. Bahaj A.S., Molland A.F., Chaplin J.R., Batten W.M.J. *Power and thrust measurements of marine current turbines under various hydrodynamic flow conditions in a cavitation tunnel and towing tank*. Renewable Energy 2006; **32** : 407-426.
18. Croft N., Pericleous K., Cross M. *PHYSICA: A multiphysics environment for complex flow processes*. Numerical Methods in Laminar and Turbulent Flows (Ed. C Taylor et al), Pineridge Press. 1995; **9** : 1269-1280.
19. Rhie C., Chow P. *Numerical study of the turbulent flow past an airfoil with trailing edge separation*. Journal of Aeronautics 1983; **21** : 1525-1532.
20. Van Dormal J.P., Raithby G.D. *Enhancements to the SIMPLE method for predicting incompressible fluid flows*. Numerical Heat Transfer 1984; **7** : 147-163.

21. Malki R., Masters I., Williams A.J., Croft T.N. *The variation in wake structure of a tidal stream turbine with flow velocity*. International Conference on Computational Methods in Marine Engineering, Lisbon, Portugal. 2011.
22. Turnock S.R., Phillips A.B., Banks P.J., Nicholls-Lee R. *Modelling tidal current turbine wakes using a coupled RANS-BEMT approach as a tool for analysing power capture of arrays of turbines*. Ocean Engineering 2011; **38** : 1300-1307.
23. Bazilevs Y., Hsu M.-C., Kiendl J., Wüchner R., Bletzinger K.-U. *3D simulation of wind turbine rotors at full scale. Part II: Fluid–structure interaction modeling with composite blades*. International Journal for Numerical Methods in Fluids 2011; **65**(1-3) : 236-253.
24. Masters I., Malki R., Williams A.J., Croft N. *The influence of turbulence model on wake structure of TSTs when used with a coupled BEM-CFD model*. Oxford Tidal Energy Workshop, University of Oxford. 2012.

Fig. 1 [a]: Schematic diagram of the discretisation of the rotor; [b]: cross-section of the blade; [c]: resolution of the lift and drag forces

Fig. 2 chord length and twist characteristics of the blade used in this study

Fig. 3 Model domain geometries and rotor layouts for [a]: single rotor; [b]: two rotors, longitudinally spaced; [c]: two rotors - laterally spaced; [d]: three rotors

Fig. 4 Normalised average wake velocity profiles downstream of a 10 m diameter rotor for different inlet velocities.

Fig. 5 Normalised average wake velocity profiles through two longitudinally spaced rotors. The location of the upstream turbine has been marked along each profile.

Fig. 6 Normalised area-mean velocities through each of the two longitudinally spaced rotors and the total power output for an inlet velocity of 3.0 m s^{-1}.

Fig. 7 Area-mean velocity profiles along the centreline between two laterally spaced rotors for a range of lateral spacings and an inlet velocity of 3.0 m s^{-1}.

Fig. 8 Contour plots of [a]: velocity and [b]: turbulence intensity for three-turbine arrays with lateral and longitudinal spacing (in diameters) of [i]: 1.5 × 1.0; [ii]: 3.0 × 1.0; [iii]: 1.5 × 10.0; [iv]: 3.0 × 10.0

Fig. 9 Velocity of the flow upstream of the downstream turbine in a three-turbine array compared to the inlet velocity. The lateral spacing of the upstream turbines are [a]: 1.5 diameters and [b]: 2.5 diameters.

Fig. 10 Velocity of the flow downstream of a three-turbine array (see Fig. 3d). The lateral spacing between the upstream turbines is 1.5 or 5.0 diameters

Fig. 11 Power output of the downstream rotor in a three-rotor array with different longitudinal (x) and lateral spacing

Fig. 12 Velocity contours for [a]: regular and [b]: modified rotor array layouts and [c]: power outputs for the two layouts

Figure 01
Click here to download high resolution image

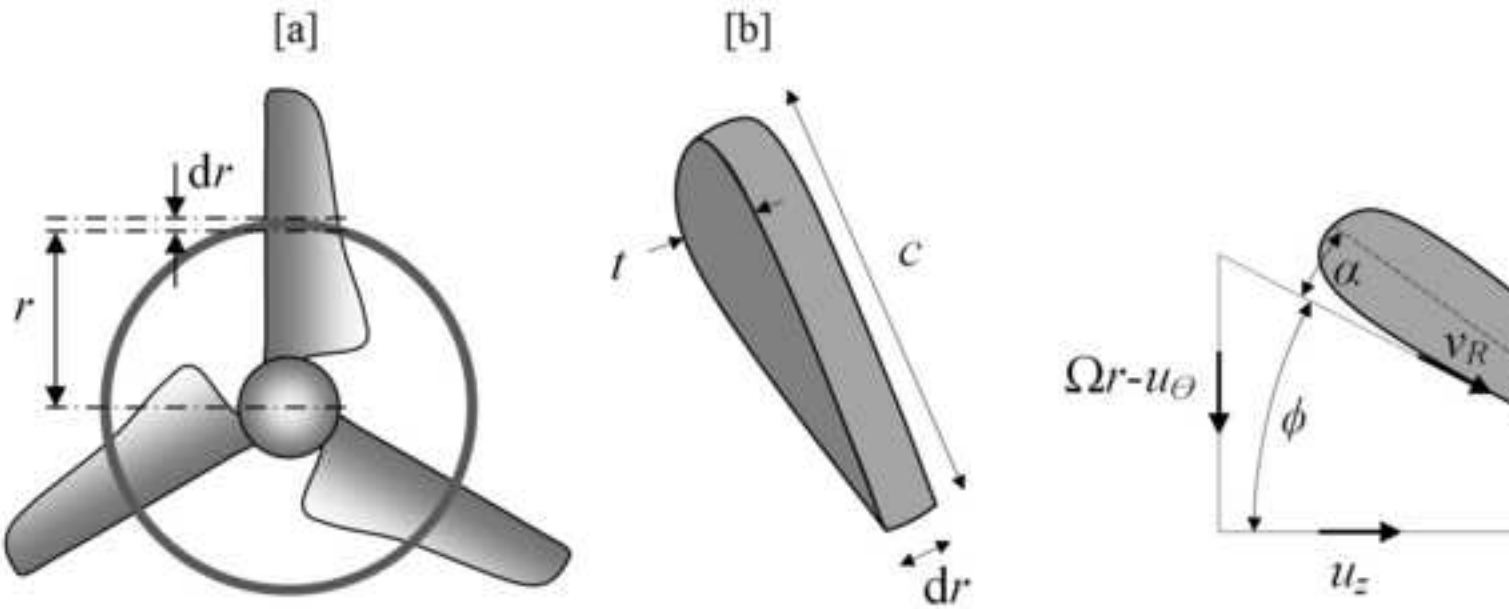

Figure 02
Click here to download high resolution image

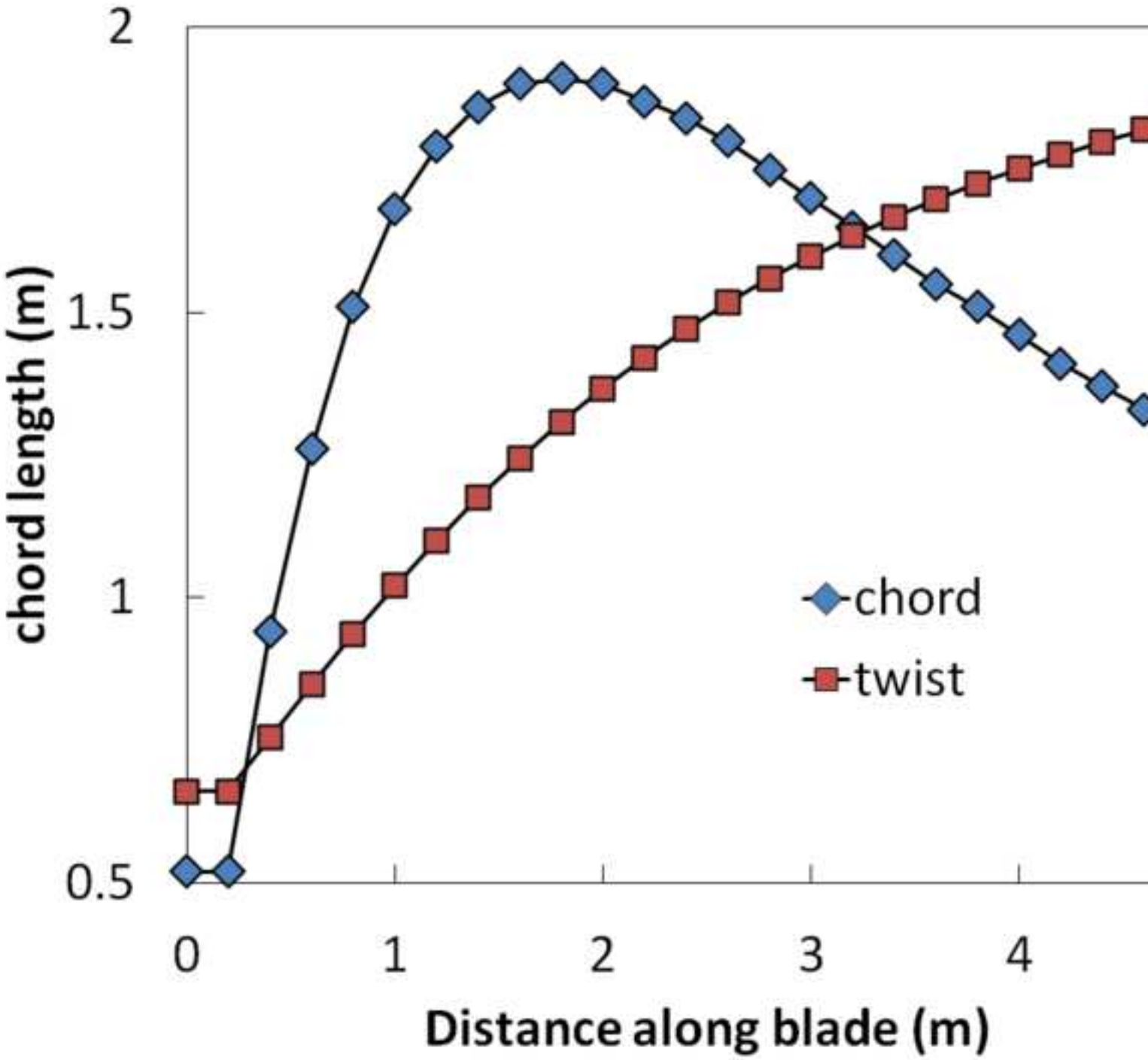

Figure 03
Click here to download high resolution image

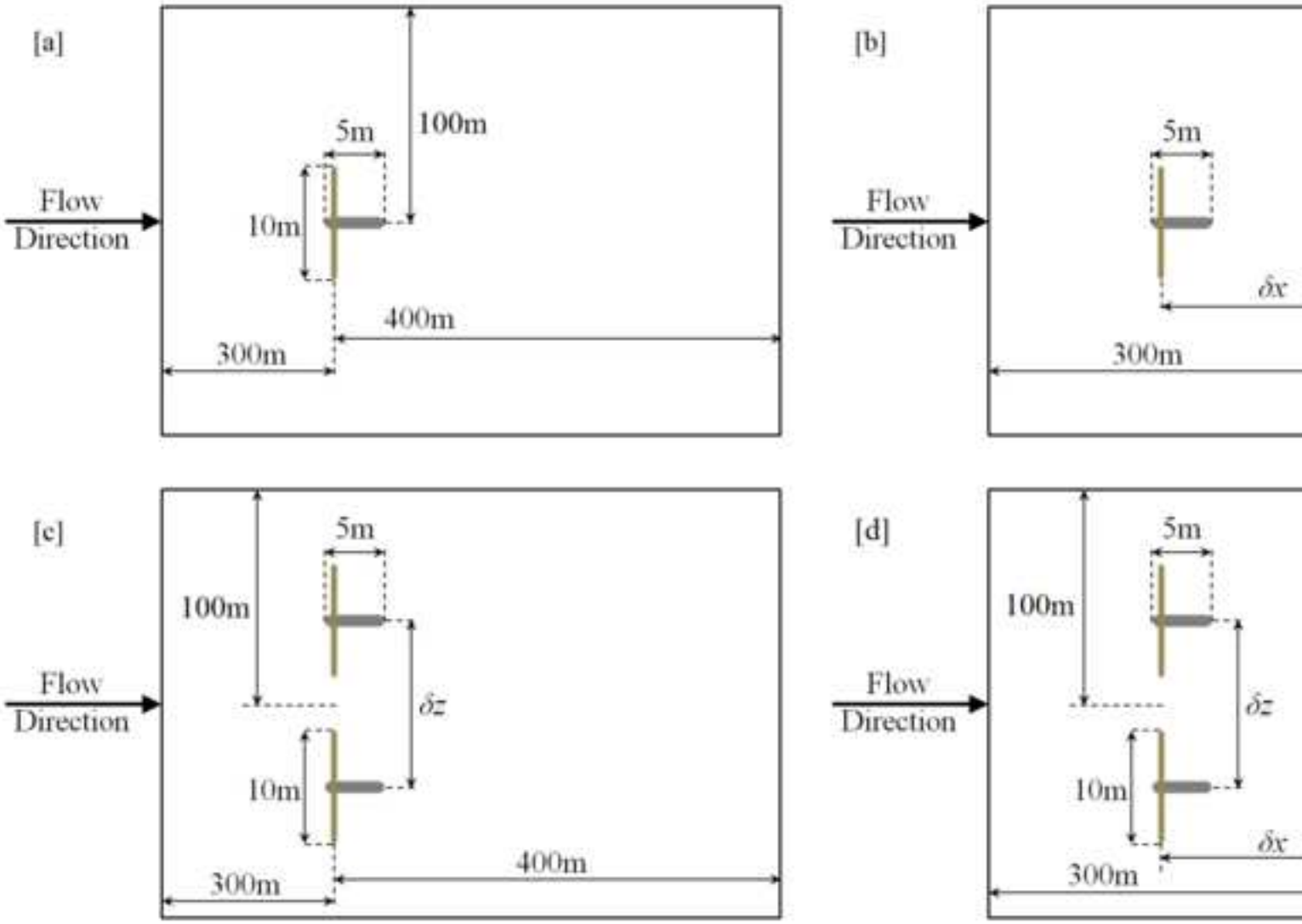

Figure 04
Click here to download high resolution image

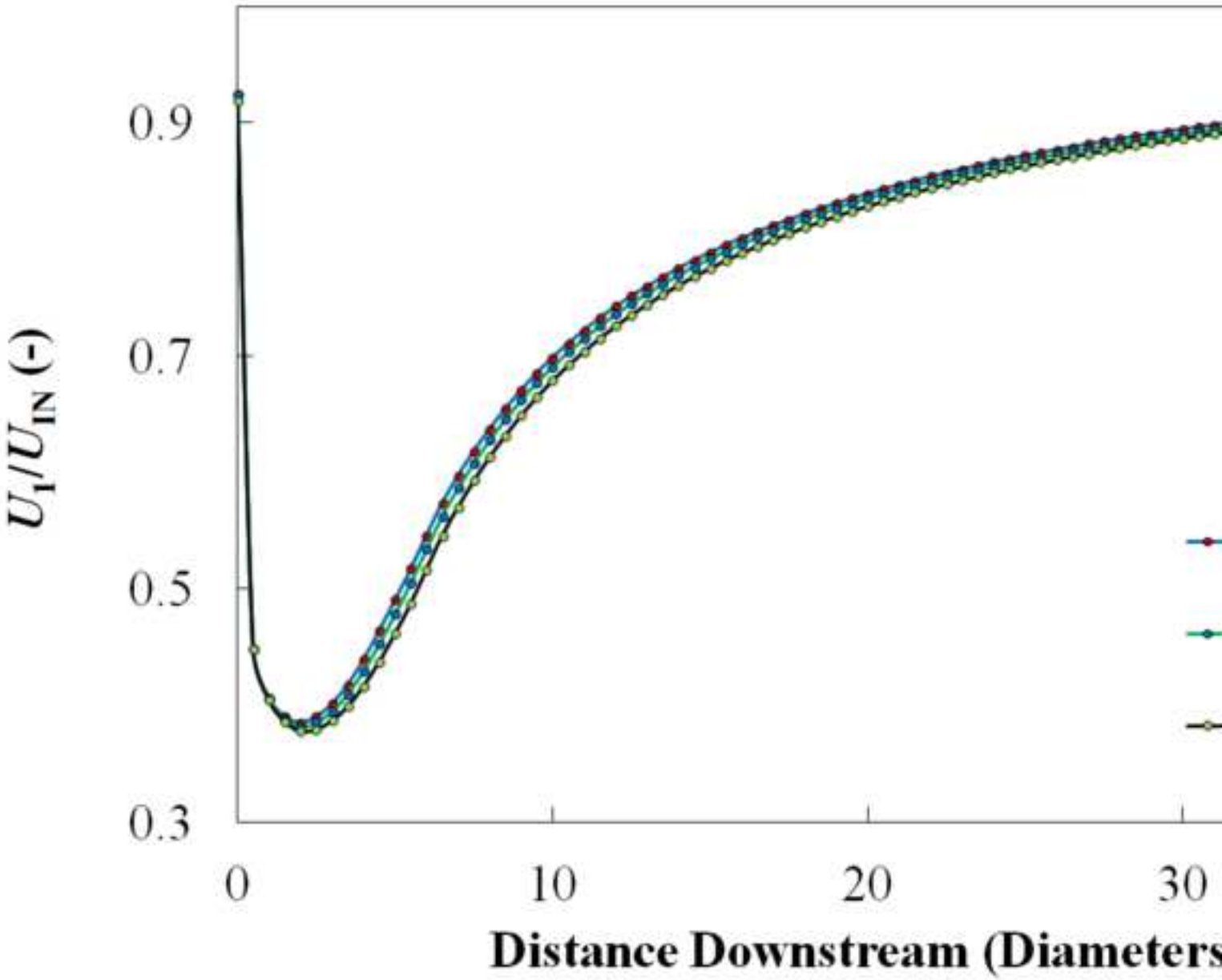

Figure 05
Click here to download high resolution image

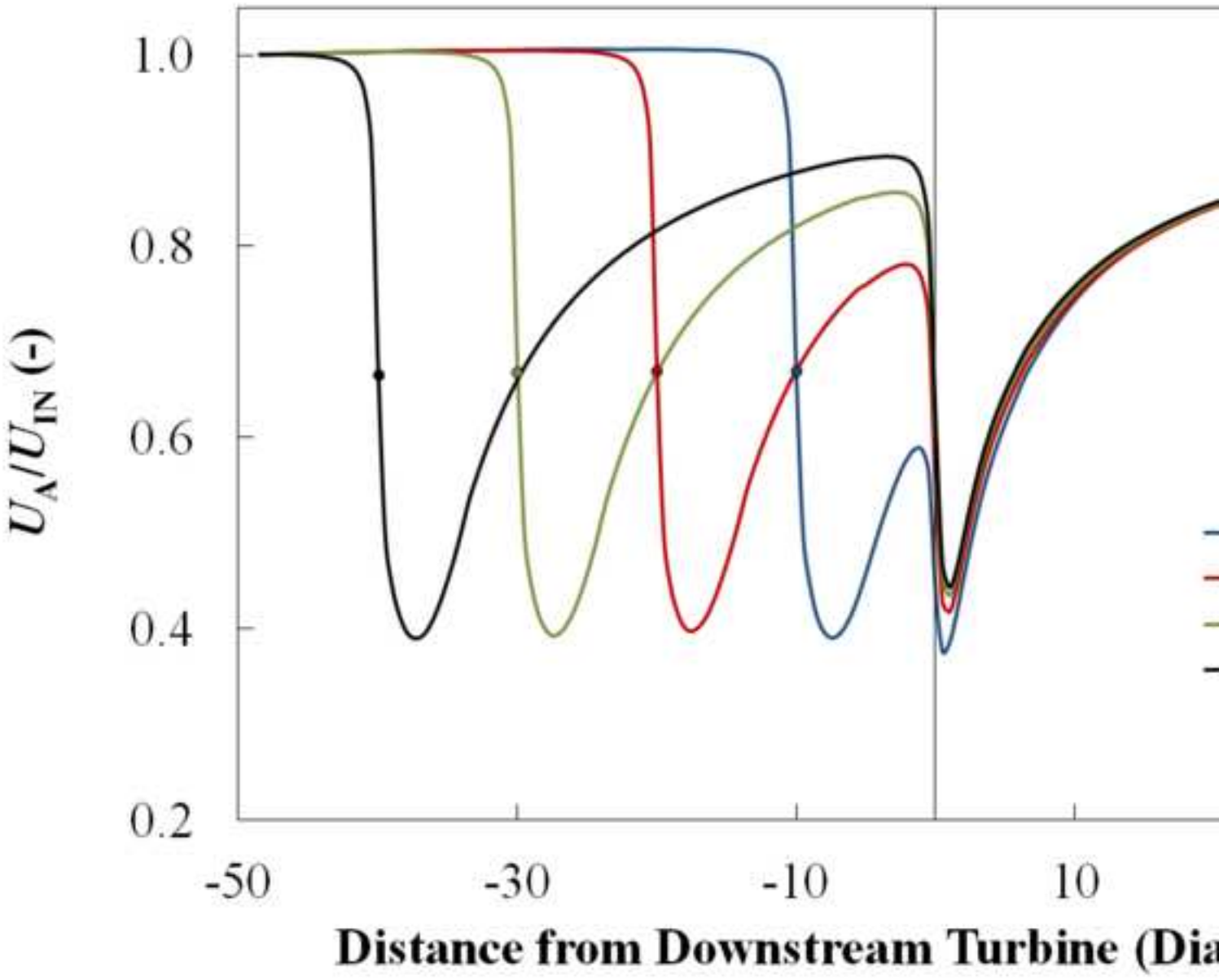

Figure 06
Click here to download high resolution image

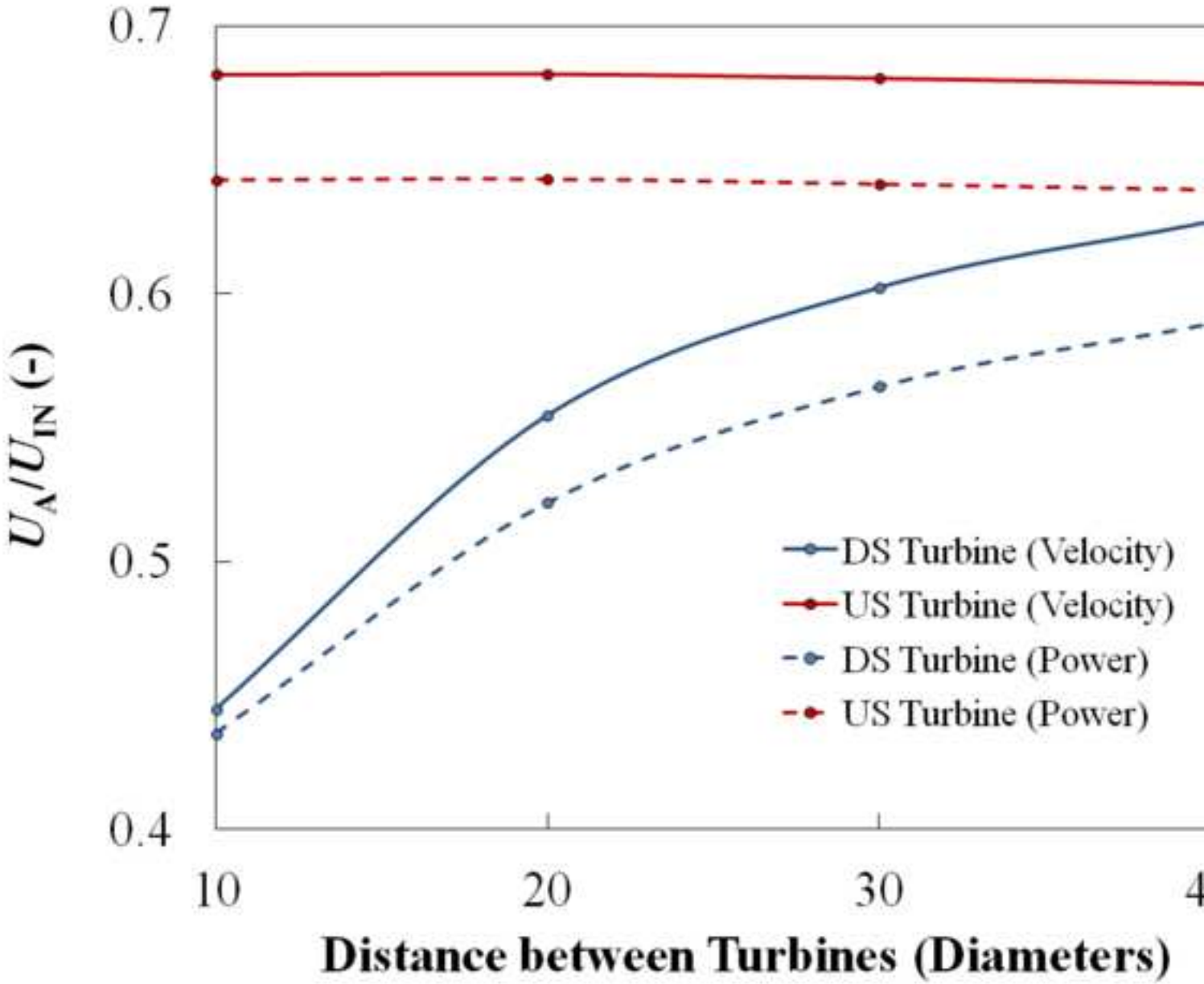

Figure 07
Click here to download high resolution image

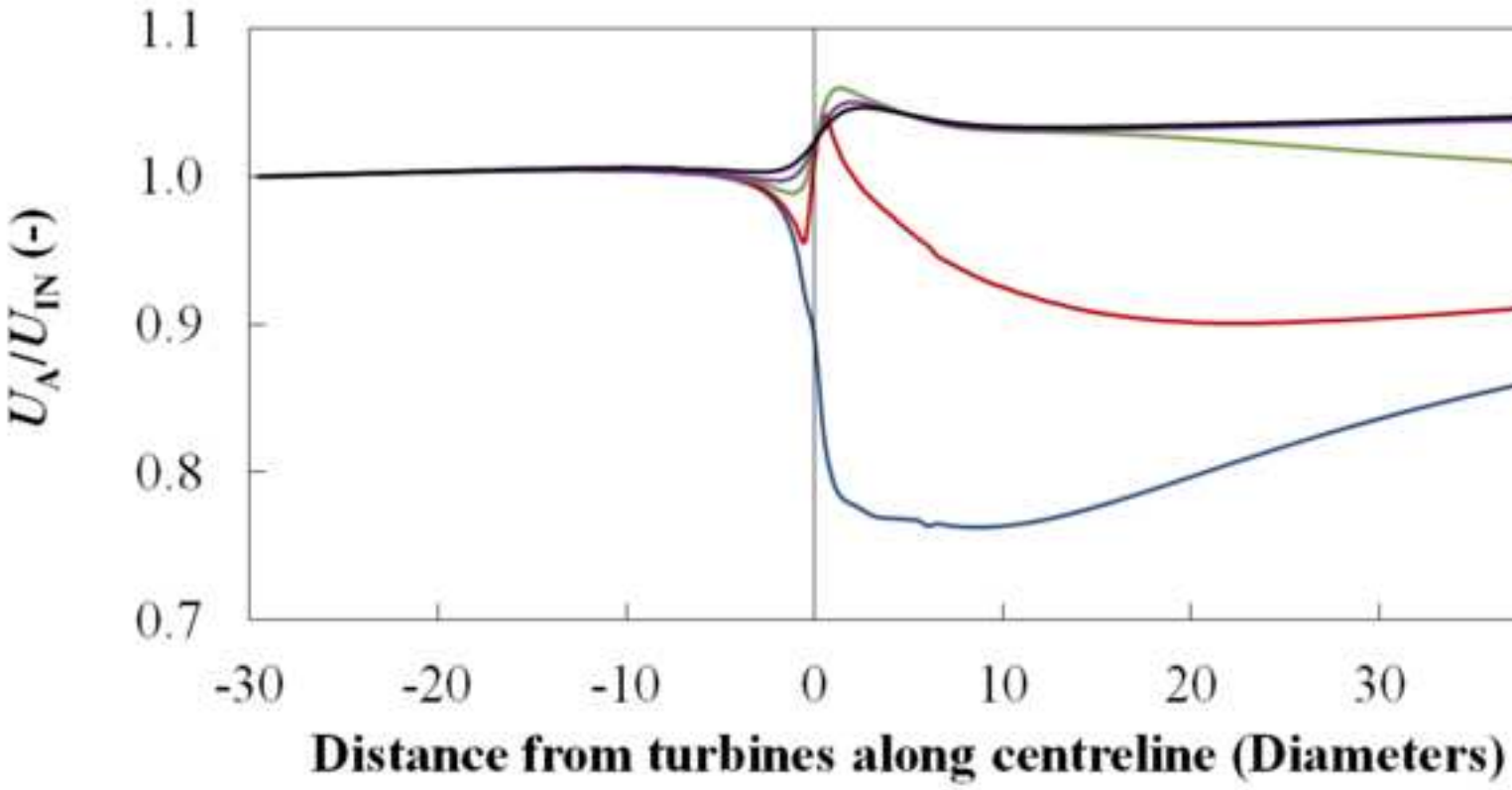

Figure 08
Click here to download high resolution image

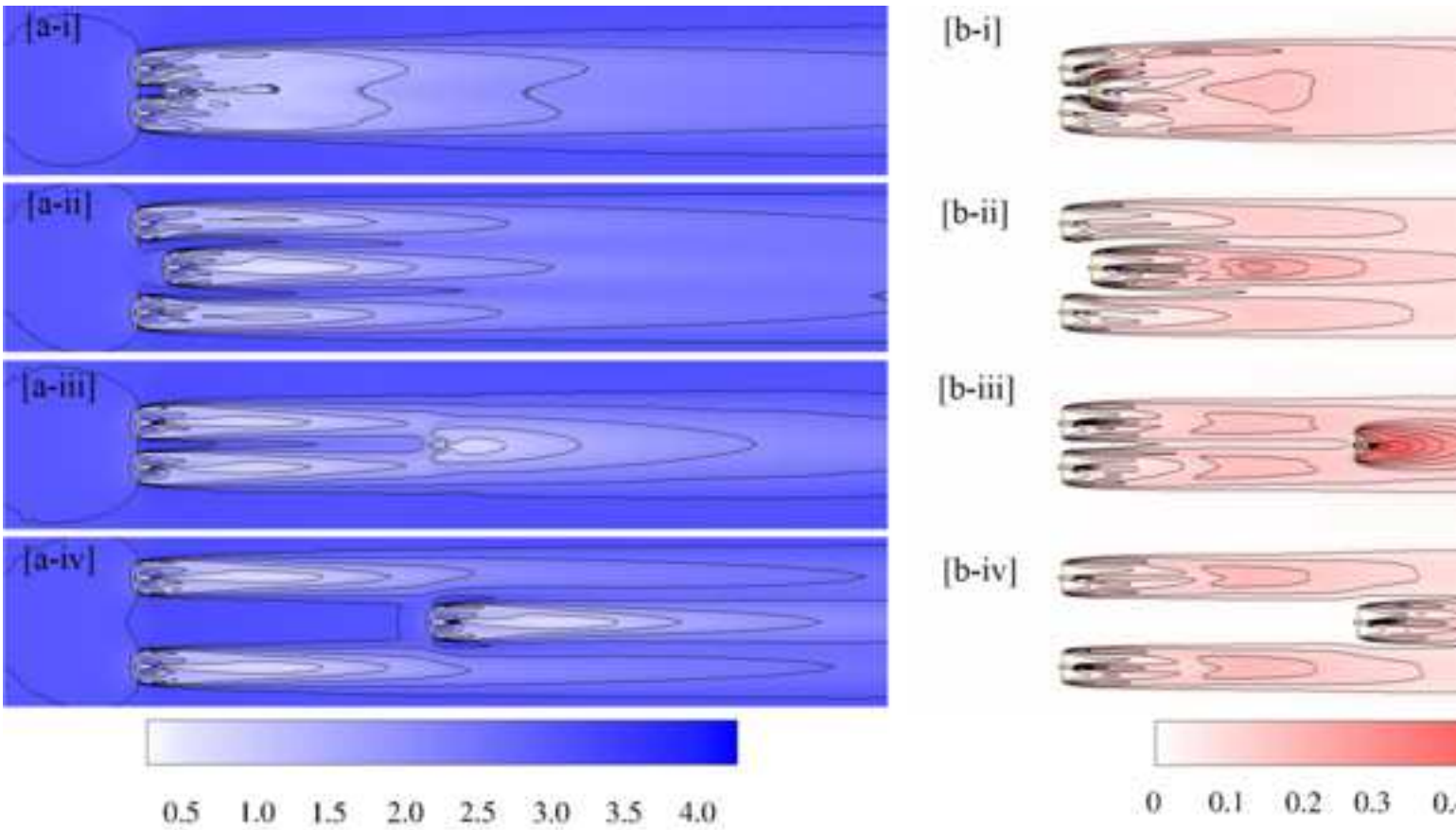

Figure 09
Click here to download high resolution image

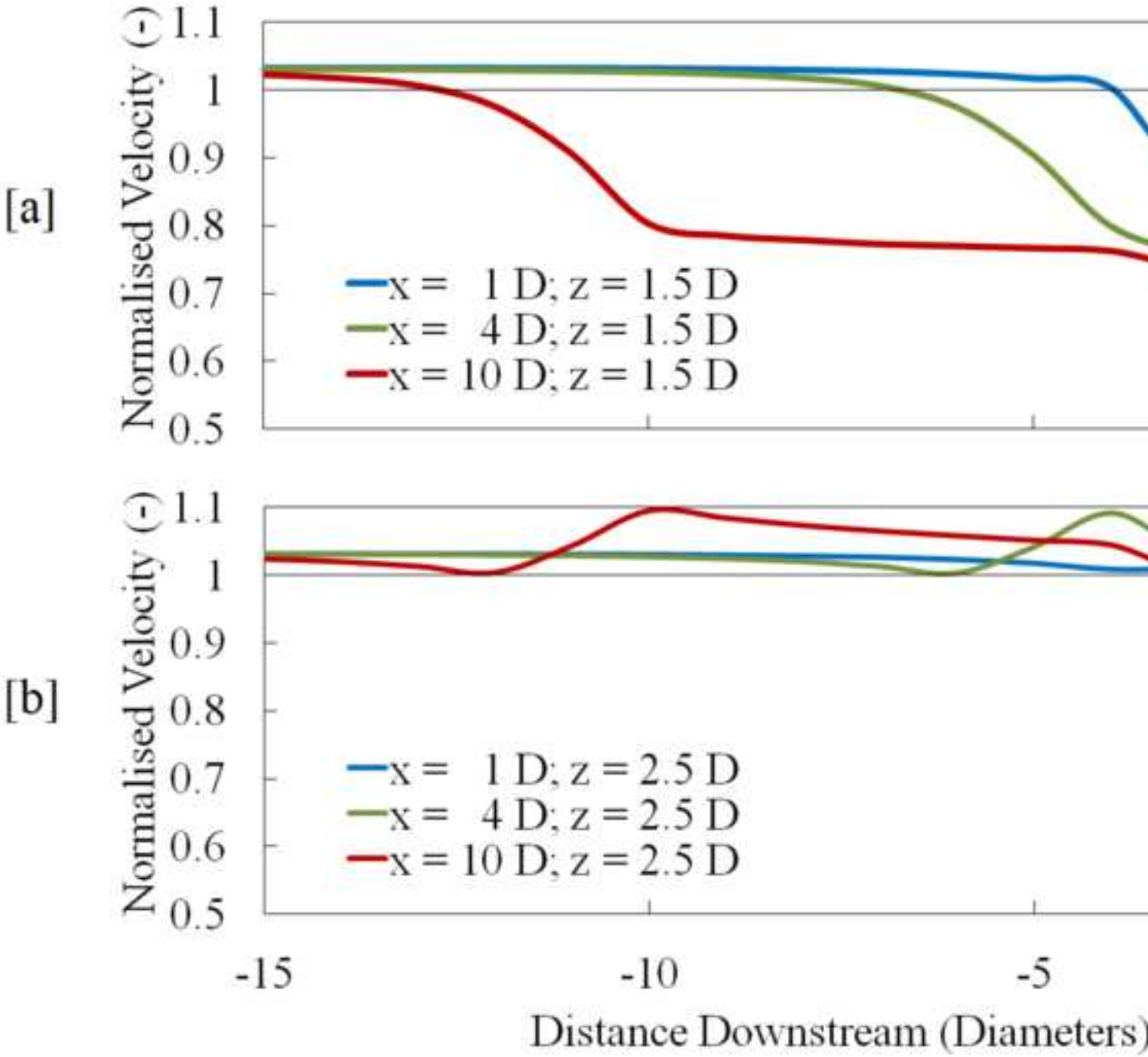

Figure 10
Click here to download high resolution image

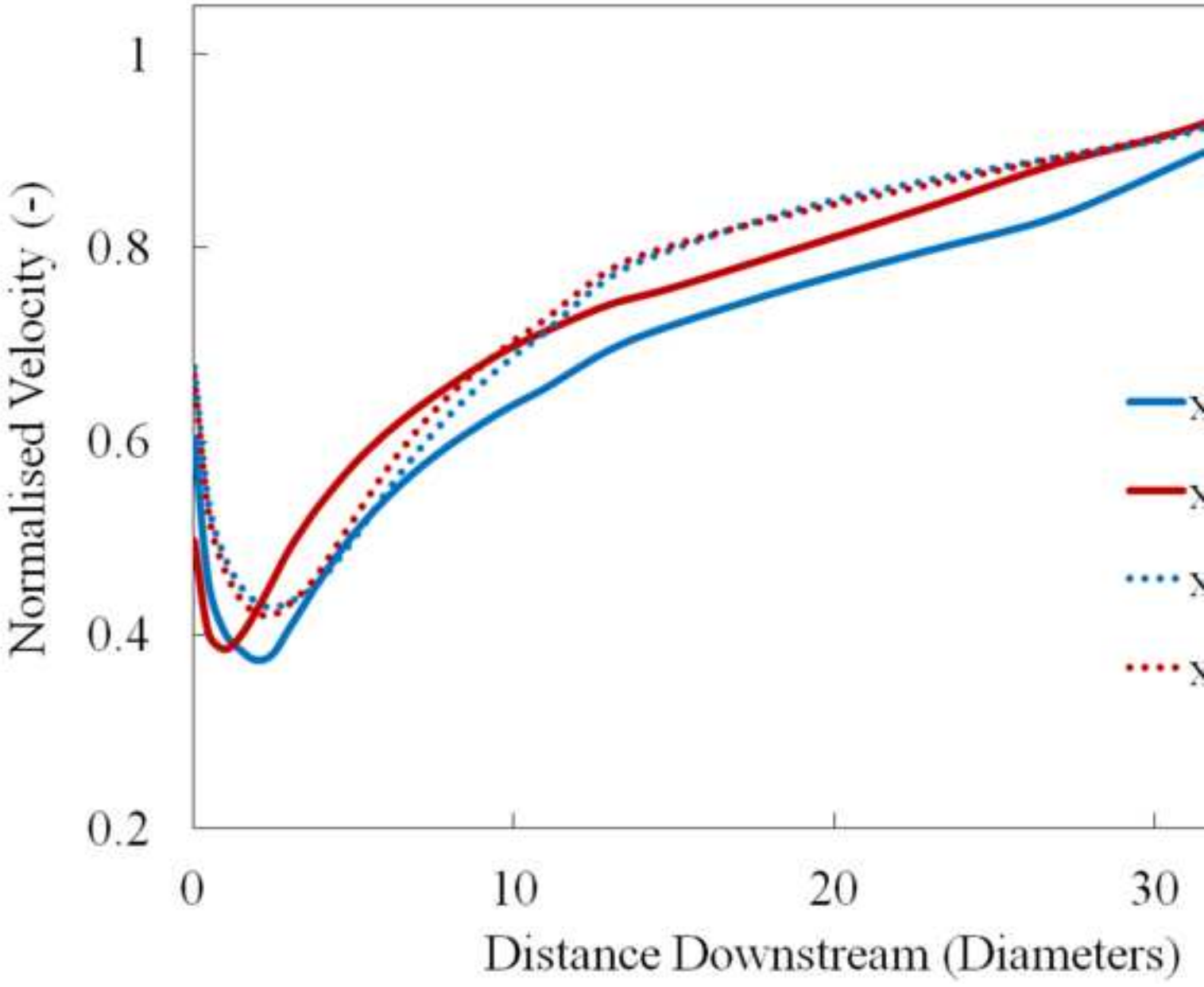

Figure 11
Click here to download high resolution image

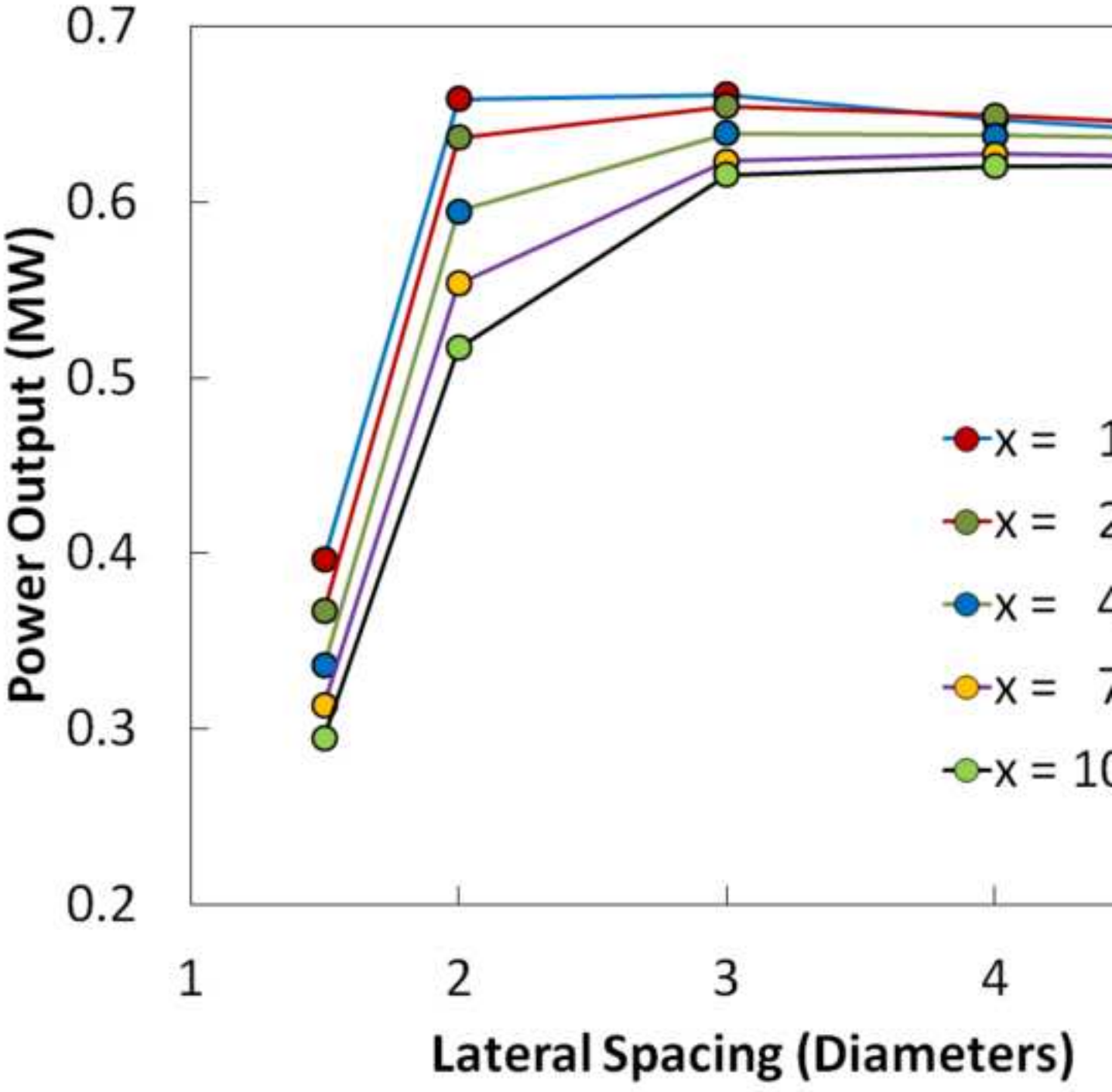

Figure 12
Click here to download high resolution image